Sustainable Energy & Fuels

ROYAL SOCIETY OF CHEMISTRY

PAPER

View Article Online
View Journal

Cite this: DOI: 10.1039/d5se01476j

The dual role of borohydride salts in enhancing perovskite solar cell performance and stability

Teresa Diaz-Perez, [ad] Carina Pareja-Rivera, [a] Jorge Pascual,[c] Hector Juarez S., [d] Sofia Masi, [*a] Eva M. Barea, [*a] Silver-Hamill Turren-Cruz [*b] and Iván Mora-Seró [*a]

Received 7th November 2025
Accepted 20th January 2026

DOI: 10.1039/d5se01476j

rsc.li/sustainable-energy

A key problem for materials that form lead-based perovskite is the part of organic iodide that is oxidized and forms molecular I_2, which negatively affects the efficiency and stability of the solar cell. Herein, we explored adding special compounds, two borohydride salts, potassium borohydride (KBH_4) and sodium borohydride ($NaBH_4$), into the perovskite precursor solution. These borohydride salts help prevent the oxidation process by acting as reducing agents, preventing the defects caused by I_2 by converting it back to I^-. Also, I_3^- is generated from I_2 and I^-, which has a strong binding affinity to FA^+, leading to deprotonation and decomposition of the perovskite. Borohydride salts can prevent this degradation and help stabilize the precursor solution. Furthermore, borohydride salts have a second role, enhancing film crystallinity and defect passivation and increasing humidity resistance, which improves overall stability and device performance. As a result, a promising efficiency of 20% is achieved, exhibiting long-term stability.

Introduction

Hybrid perovskite solar cells (PSCs) have attracted significant attention in recent years due to their remarkable efficiency and enhanced stability, making them a primary focus of current research.[1–3] These performance improvements are primarily attributed to key advances in additive engineering,[4] interlayers, passivation,[5] cation mixing,[6] ion migration in mixed halides[7,8] and phase segregation to improve environmental stabilization.[9] Despite these notable developments, PSCs still face significant challenges related to material degradation, particularly under real-world operating conditions.[10,11] Recent studies have highlighted that a critical point of instability originates in the perovskite precursor solution, where chemical reactions can alter the intended composition of the perovskite and negatively impact the quality of the final material. During storage or preparation, degradation products such as molecular iodine (I_2) and triiodide (I_3^-) can form due to the oxidation of iodide.[12] These species are highly detrimental to the film's crystallinity and purity and can significantly reduce device efficiency and long-term stability. This degradation is by deprotonation of the FA^+ cation, which releases protons that then react with iodide ions to generate I_2.[13] The presence of molecular iodine and other iodine-related defects introduces trap states in the material, negatively affecting charge transport and accelerating performance loss over time.[14] Furthermore, the degradation of the precursor solution leads to harmful film morphology, reduced grain size, increased defect density, and phase instability. For this reason, an effective strategy to prevent perovskite degradation could be the use of borohydride salts such as KBH_4 and $NaBH_4$ as additives. We explored these compounds, which act as both reducing agents and weak bases, and suppress the formation of I_2. In addition to stabilizing the precursor solution, borohydride salts have been shown to improve film crystallinity, reduce defect density, and enhance moisture resistance, ultimately resulting in more efficient and longer-lasting perovskite solar cells.

Researchers have explored strategies such as defect passivation engineering and reducing agents to address this issue, which have shown great promise in mitigating degradation.[15–18] Several studies have successfully employed chemical additives in tin-based perovskite cells to stabilize the material, particularly by reducing Sn^{4+} formation. Tin tends to oxidize from Sn^{2+} to Sn^{4+}, a process that leads to structural degradation and defect formation in the perovskite film. The incorporation of $NaBH_4$, for instance, not only effectively suppresses this oxidation but also significantly enhances device stability.[19] Although Pb does not have the same tendency to oxidation than Sn, oxidation process occurs in lead-based perovskites, where iodide (I^-) oxidizes to molecular iodine (I_2), it is proposed that $NaBH_4$ could provide similar benefits. Its use in lead-based perovskites

[a]Institute of Advanced Materials (INAM), University Jaume I, Av. Vicent Sos Baynat, s/n, 12071, Castellón de la Plana, Spain. E-mail: masi@uji.es; barea@uji.es; silver.turren@uv.es; sero@uji.es

[b]Instituto de Ciencia de los Materiales (ICMUV), Universitat de Valencia, 46980 Paterna, Spain. E-mail: silver.turren@uv.es

[c]Polymat, University of the Basque Country UPV/EHU, 20018 Donostia-San Sebastian, Spain

[d]Centro de Investigación en Dispositivos Semiconductores, Benemérita Universidad Autónoma de Puebla, 14 Sur and Av. San Claudio, San Manuel, 72000, Puebla, Mexico

may help stabilize the material, reduce defect formation, and ultimately improve the performance and operational stability of the devices. A recent study by Wu *et al.* highlights the use of the ionic salt sodium borohydride ($NaBH_4$) as an interfacial modifier between HTL and perovskite, addressing the defects commonly found at this interface. The incorporation of $NaBH_4$ improved interfacial energy alignment and significantly reduced interfacial defects in inverted perovskite solar cells, leading to enhanced device performance.[20] These strategies show great potential for improving lead-based perovskite solar cells' long-term stability and efficiency, supporting their future commercialization.

Another recent study by Liu *et al.* explored the incorporation of the ionic salt potassium borohydride (KBH_4) as a reducing agent at the NiO_x/perovskite interface, effectively suppressing the harmful formation of Ni^{4+} and preventing iodide oxidation in inverted nickel oxide (NiO_x)-based perovskite solar cells.[21] These results suggest that borohydride salts have successfully improved interface stability and could similarly benefit lead-based perovskites. By acting as reducing agents, borohydrides could suppress I_2 formation, mitigate defect generation, enhance the film quality, and ultimately improve device performance. Other strategies that have been employed in the addition of additives for the degradation of perovskite in the precursor solution are Chen *et al.*, who introduced benzylhydrazine hydrochloride (BHC), which converts harmful I_2 back into I^-, reducing I_3^- charge traps and restoring precursor quality.[22] Similarly, the additive potassium tetrafluoroborate (KBF_4) has been reported to enhance inverted perovskite solar cells by reducing microstrain, improving crystallinity, and passivating defects. This optimization led to improving stability and resistance to degradation.[23–25] Conversely, Duan *et al.* reported $CsPbI_3$ perovskite solar cells using 4-fluorobenzothiohydrazide (FBTH) in the precursor solution. FBTH enhances stability by preventing I_2 formation and suppressing I^- migration through strong N–H···I bonds. It also passivates lead-related defects *via* S···Pb interactions, reducing trap states and improving charge dynamics and stability under thermal and light exposure.[26]

This research has significantly improved the stability and performance of perovskite materials, but further research is still needed for their large-scale commercialization. In this work, we focus on investigating two ionic borohydride salts, sodium borohydride ($NaBH_4$) and potassium borohydride (KBH_4), as effective reducing agents to enhance device performance. Both additives exhibit good solubility in organic solvents and beneficial chemical properties. Notably, $NaBH_4$, due to its stronger ionic interactions and higher reducing power compared to KBH_4, is more effective at suppressing iodide oxidation, minimizing defect formation, and improving the film quality, leading to increased efficiency and long-term stability of perovskite solar cells.

Herein, we present the optimization and analysis of $Cs_{0.1}FA_{0.9}PbI_3$ ($CsFAPbI_3$) perovskite precursor solutions, with and without adding two reducing agents, $NaBH_4$ and KBH_4. Our study initially focused on understanding the role of these reducing agents in preventing the oxidation of precursors within the solution, specifically by reducing iodine (I_2) to iodide (I^-). The main finding was that these agents stabilize the precursor solution and enhance stability in the solid state by passivating surface defects. This effect was confirmed by fabricating and characterizing solar cells made of perovskite with and without additives, demonstrating the beneficial impact of the reducing agents. Incorporating the additives KBH_4 and $NaBH_4$ enhances the properties of the perovskite films by increasing their crystallinity and grain size, effectively passivating defects, and minimizing non-radiative recombination.

Results and discussion

The processes occurring in a perovskite precursor solution by iodine-related defects resulting from borohydride can effectively eliminate these defects, as schematized in Fig. 1. This reaction stabilizes the precursor solution, reducing defects and improving the quality of the perovskite films. The result is a stable perovskite structure with fewer non-radiative recombination centers to enhance the efficiency and longevity of the devices.[27] To study the oxidation of I^- to I_2, a pristine Formamidinium Iodide (FAI) solution was prepared and analyzed by UV-vis spectroscopy, see Fig. 2a. Two additional solutions were prepared, one with the addition of KBH_4 (0.05 mg mL^{-1}, 0.93 mM) and another with $NaBH_4$ (0.05 mg mL^{-1}, 1.32 mM) as reducing agents, see Fig. 2b and c, respectively. The solutions had been aged in the air for 6 hours. The absorbance spectrum exhibits a characteristic increase of absorption at 365 nm region, indicating the oxidation of I^- to I_2 in the FAI solution. In contrast, with borohydride solutions, the absorbance does not change significantly.

The main degradation mechanism is oxidation iodide (I^-) when exposed to air, moisture, or illumination, which triggers the following reaction eqn (1):[28–30]

$$2I^- \rightarrow I_2 + 2e^- \quad (1)$$

This process leads to the decomposition of PbI_2 or halide loss. The borohydride ion (BH_4^-) donates electrons to the oxidized species (I_2) in the precursor solution or in the film, reacting as follows eqn (2):

$$I_2 + 2BH_4^- + 2H_2O \rightarrow 2I^- + 2B(OH)_3 + 3H_2\uparrow \quad (2)$$

This allows I_2 to be reduced back to I^-, restoring the stable halide state within the perovskite structure. This means that both additives can reverse the oxidation process. In addition, BH_4^- can coordinate with Pb^{2+} improving the interface between ETL and perovskite layer.[20]

Another experiment of the absorption was measured immediately after preparation and then daily for up to 5 days. It was conducted by varying molar proportions of borohydrides (0.05, 0.1, 0.2, and 0.3 mg mL^{-1}) added to the FAI precursor solution, see Fig. S1. After 5 days of aging in air, a similar trend was observed KBH_4 and $NaBH_4$, where significant oxidation of I^- occurred only in the sample without borohydrides. The optical appearance of the solutions aging FAI and with and

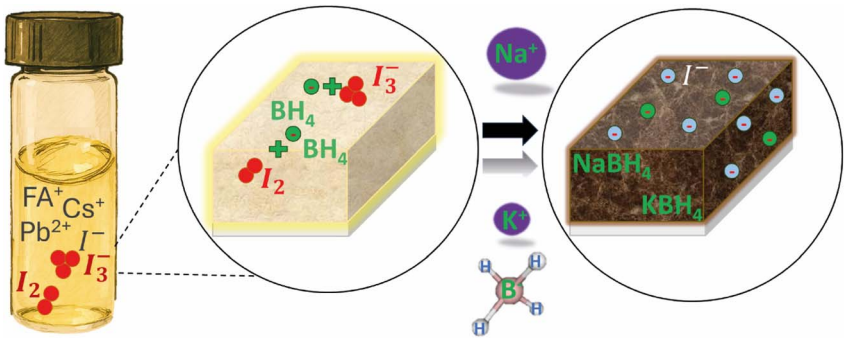

Fig. 1 Schematic illustration of I_3^- oxidation and generation during the aging of the perovskite precursor solution and the influence of sodium or potassium borohydride incorporation on perovskite solution.

without borohydrides can be observed in Fig. S1f. The FAI solution has a light-yellow color, while this yellowish color is not observed with the borohydride solutions. Furthermore, another experiment demonstrated that FAI solution was exposed in air and clearly exhibited the formation of I_2 (Fig. S2). However, borohydride additive was added to aged FAI solution and the yellow color disappeared immediately. The solution regained its transparent appearance confirming that I_2 was reduced to I^-.

This effect clearly demonstrates that both $NaBH_4$ and KBH_4 can reduce I_2/I_3^- species in the perovskite precursor solution. We therefore propose that borohydride additive acts reduce oxidized I_2 species in the perovskite precursor. Furthermore, demonstrate suppress generation of I_2 within perovskite film by increasing absorbance enhances charge carrier capture in the presence of borohydrides.

To investigate the effect of KBH_4 and $NaBH_4$ on the perovskite film morphology, we used scanning electron microscopy (SEM). Fig. 3a presents images of perovskite fresh films for both reference and samples with KBH_4 and $NaBH_4$. The reference film exhibits small, non-uniform grains. In contrast, adding KBH_4 and $NaBH_4$ results in films with more homogeneous and improved grain distribution. This significant increase in the film treated with $NaBH_4$ indicates an average grain size of 960 nm, 720 nm for the potassium-treated film, and 630 nm for the reference film in the statistical graph of grain size, see Table S1. Bigger grain size and homogeneous film can potentially reduce defects, enhance transport charge carriers, and improve the solar cell's performance. To analyze the long-term effect additives in the morphology of perovskite films, morphology was also analyzed after 3 months of aging, see Fig. 3b. During the aging time the films were stored under dark in a dry box at 20% RH and 25 °C. The aged perovskite films show holes in the case of reference and KBH_4 films. In contrast, with $NaBH_4$, there are no holes or defects on the surface of aged samples. However, it is observed an a slight increase in the average grain size after aging, see Table S1, but considering the standard deviation, it cannot be concluded that this increase is statistically significant.

X-ray diffraction (XRD) patterns of fresh and aged $CsFAPbI_3$ perovskite film are plotted in Fig. 4a. The perovskite film incorporating $NaBH_4$ exhibits stronger diffraction peaks compared to the other films, pointing to enhanced crystallinity.

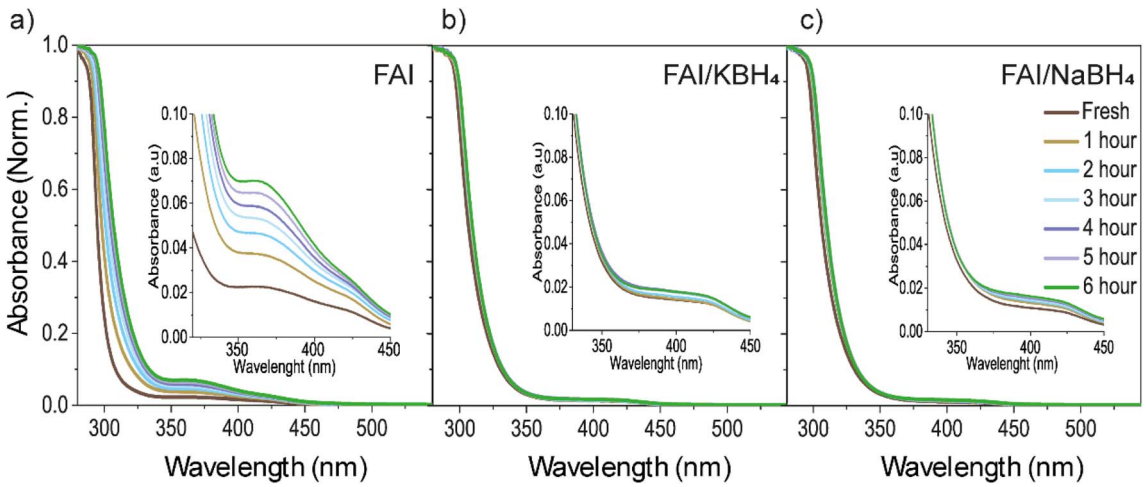

Fig. 2 UV-Vis absorption spectra of solutions: (a) FAI, (b) FAI/KBH_4, and (c) $FAI/NaBH_4$ (0.05 mg mL^{-1}) in DMF : DMSO (4 : 1 v/v) solvent mixture. The spectra were recorded after 6 hours of aging in air. The FAI solution exhibits a characteristic peak at 365 nm, indicating iodine oxidation.[12–22] In contrast, aged solutions KBH_4 and $NaBH_4$ show similar absorbance effects without signs of oxidation.

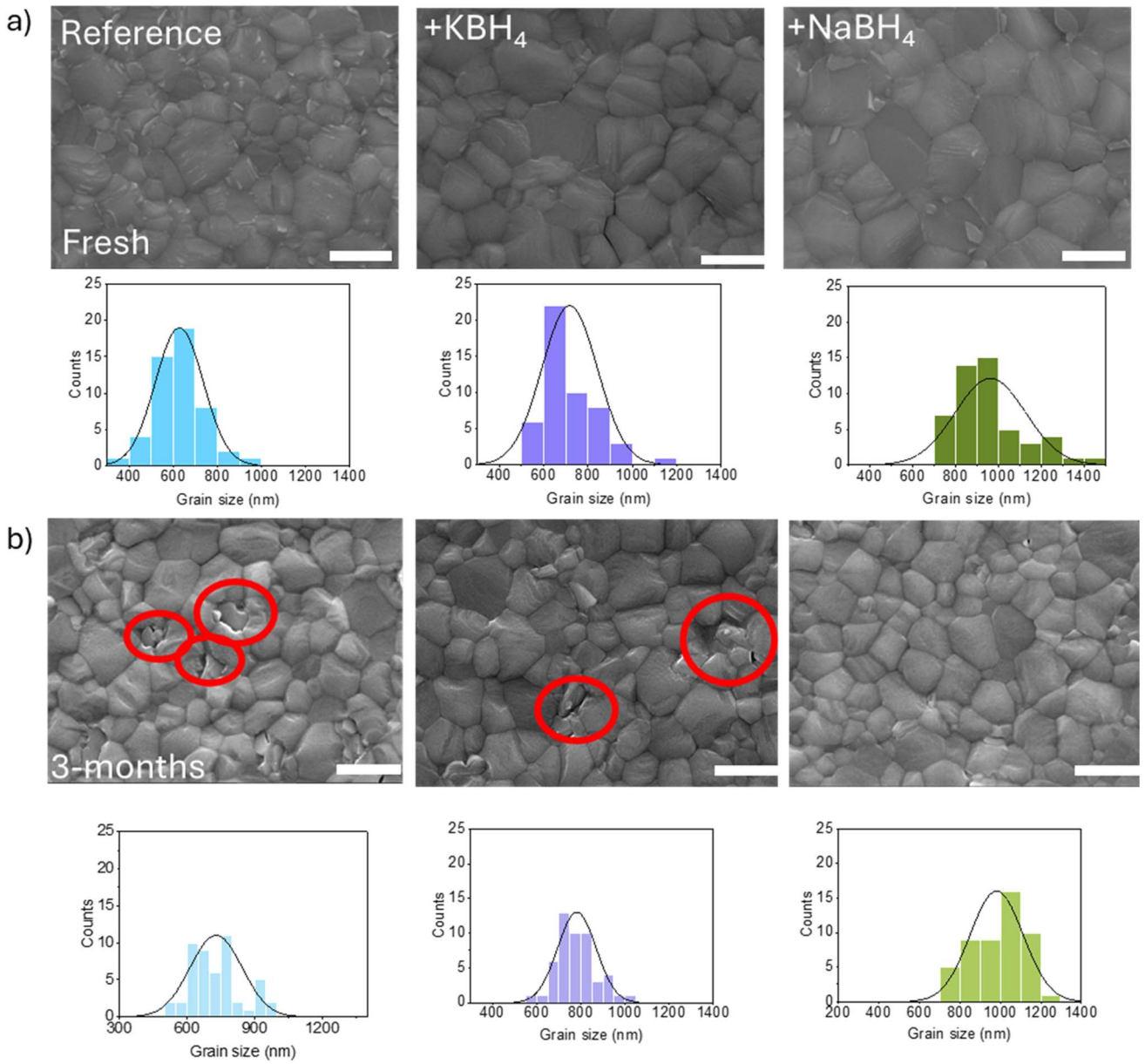

Fig. 3 Top-view scanning electron microscope (SEM) images of films and histogram of grain size extracted from the views. (a) Reference perovskite type $CsFAPbI_3$, with $+KBH_4$, and with $+NaBH_4$ (0.05 mg mL^{-1}) on glass substrates. (b) 3-Month films of aging in the dry box at 20% RH and 25 °C. The scale bar corresponds to 1 μm. Red circles highlight pinhole regions.

No new peaks are observed in the XRD patterns after adding borohydrides. The degradation of the perovskite films is evident with the appearance of a δ-FAPI peak at 11.80° after 3 weeks of aging. Nevertheless, the control and KBH_4 films display this peak more intensely than the $NaBH_4$ film, suggesting a more effective defect passive way to grain boundaries and interfaces. The observed diffraction peaks are 13.95°, 19.85°, 24.30°, 28.10°, 31.50°, 34.65°, 40.25° and 42.75°, corresponding to (1 1 0), (1 1 2), (1 1 1), (2 0 0), (2 1 0), (2 1 1), (2 2 0) and (2 2 1) of the cubic perovskite alpha black phase.[31]

In the study by Ho *et al.*, it was shown that individual grains undergo chemical and structural changes during light- and humidity-induced degradation or phase segregation in mixed-cation perovskites. Importantly, they demonstrated that the degradation pathways differ depending on the stress conditions. Under light exposure, nanoscale depressions were observed to form over time, whereas under high relative humidity such depressions were not necessarily detected; instead, grain coarsening and growth were observed. Based on these observations, Ho *et al.* suggested that the formation of surface depressions is primarily light-driven and can be accelerated by higher relative humidity.[32]

In our case, although the aging was performed under relatively low humidity and in the absence of illumination, similar early-stage degradation processes such as phase transformation decomposition pathways may still occur within the bulk or at

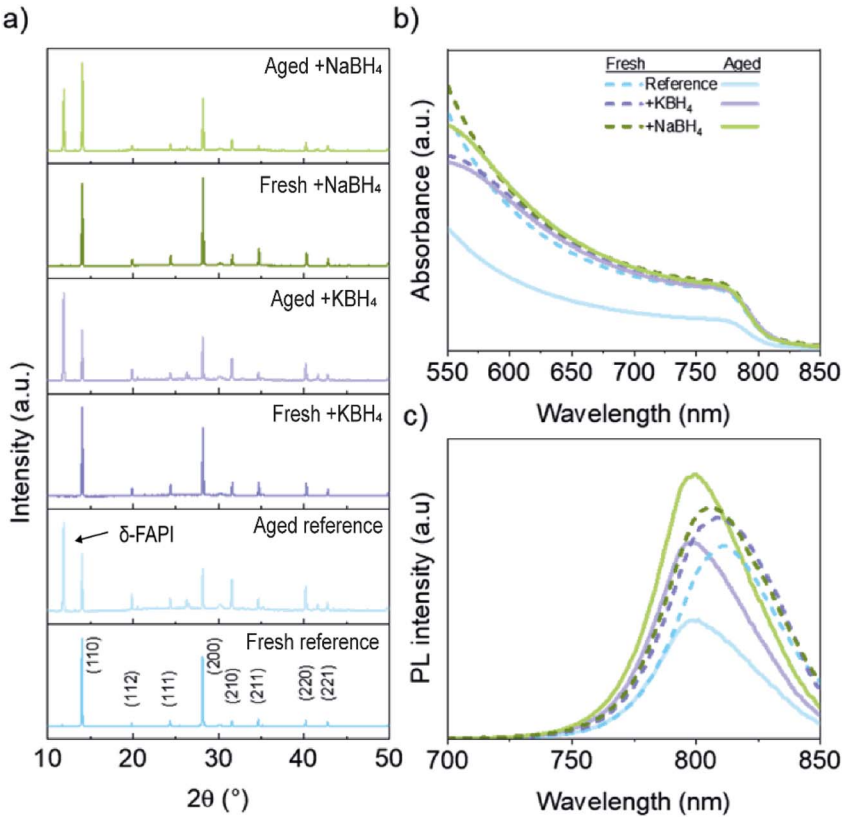

Fig. 4 Perovskite type $Cs_{0.1}FA_{0.9}PbI_3$ films with/without KBH_4 and $NaBH_4$ (0.05 mg mL^{-1}) on glass substrates. (a) XRD fresh/aged films and aged, (b) UV-Vis absorption, and (c) PL spectra fresh and PL after 3 months of aging (20% RH and 25 °C).

grain boundaries. These processes can lead to structural changes detectable by techniques sensitive to crystallographic without necessarily producing pronounced morphological changes observable. Therefore, the absence of obvious surface degradation in SEM images does not preclude underlying structural degradation, particularly under mild aging conditions, and is consistent with the degradation mechanisms reported for mixed-cation perovskites.

The UV-vis light absorption spectra of perovskite films are then shown in Fig. 4b. The fresh perovskite films with and without additives show similar light absorption intensity. However, after 3 months, the reference sample showed low absorption intensity due to the film's degradation, and the massive formation $FAPbI_3$ yellow delta phase, as shown in the XRD measurements, see Fig. 4a. Despite δ-FAPI is also detected in the XRD measurements in aged samples with borohydrides, the amount of degraded material is significantly lower than in fresh samples, as no significant reduction is light absorption is detected, see Fig. 4b. In the study by Kang D. H. *et al.* have shown that absorbance of perovskite films is relatively insensitive to small amounts of PbI_2 formation, particularly when PbI_2 is present in excess at low concentrations. In such cases, almost no change in optical absorbance is observed, even though XRD clearly reveals the presence of secondary phases. In contrast, a pronounced decrease in absorbance is typically associated with the formation of the non-perovskite δ-phase, which is optically inactive in the visible region and can be readily confirmed by XRD through the appearance of intense δ-phase diffraction peaks. This behavior highlights that structural degradation detected by XRD can precede or occur independently of significant optical degradation, especially when the degradation pathway involves PbI_2 formation rather than extensive δ-phase conversion. This behavior highlights that structural degradation detected by XRD can precede or occur independently of significant optical degradation, especially when the degradation pathway involves PbI_2 formation rather than extensive δ-phase conversion.[33] Therefore, in our case, the preserved absorption intensity with borohydride films after aging indicates that it remains largely intact. In contrast, the XRD results reveal underlying phase evolution and clearly indicate the formation of secondary phases, that do not yet translate into a measurable loss of optical absorption.

Moreover, the steady-state photoluminescence (PL) was performed on perovskite films with different borohydrides, as shown in Fig. 4c. The fresh film shows that PL increases with borohydride additives respect the reference, pointing for a beneficial role reducing the non-radiative recombination. Note that there is a blue shift of the PL peak after aging, see Fig. S3, due to the higher relative Cs amount of respect FA in the $CsFAPbI_3$ perovskite due to the formation of δ-FAPI. In addition, after 3 months, PL even increases for films with $NaBH_4$ additive. A high open circuit steady state PL indicates lower non-radiative

recombination in the film, attributed to fewer defect density.[31,34,35] In contrast, in reference and KBH_4 films aged over time, the PL intensity of perovskite films decreases, likely due to defects generated during the aging as observed in SEM with the aged films, see Fig. 3b. Ma, F. *et al.* demonstrated that the presence of an α/δ phase junction induces a spectral shift in the photoluminescence (PL) emission and, importantly, can result in enhanced PL intensity compared to a pure α-phase film. This enhancement is attributed to a reduction in nonradiative recombination, likely due to defect passivation and improved interfacial energetics at the phase junction, which suppress trap-assisted recombination.[36] Therefore, in our case, although XRD indicates structural degradation and phase evolution after prolonged aging, the increased PL intensity observed for the $NaBH_4$ perovskite film can be rationalized by the formation of a mixed α/δ phase configuration. This phase mixture can reduce nonradiative losses and enhance radiative recombination efficiency, leading to stronger PL emission despite the presence of secondary phases.

After film analysis and characterization complete perovskite solar cell devices were fabricated with an N–I–P configuration of glass|ITO|SnO_2| perovskite ($NaBH_4$ or KBH_4) |Spiro-OMeTAD| Au, see Fig. 5a. The statistical parameters of the cells are shown in Fig. 5b, including open circuit potential, V_{OC}, short circuit current, J_{SC}, fill factor, FF, and photoconversion efficiency, PCE. The device's performance corresponds to devices after 3 months aging, stored under dark in a dry box at 20% RH and 25 °C. It is observed that the cell with the best photovoltaic performance after aging time is the $NaBH_4$-based cell, achieving a maximum PCE of 18.9%, followed by 17.7% for the KBH_4-based cell and 15.5% for the reference cell. This fact is in good agreement with film aging characterization of $NaBH_4$ samples that showed lower δ-FAPI content, see Fig. 4a, and good film morphology, see Fig. 3b, and higher PL, see Fig. 4c, pointing to a decrease superficial defect with a non-radiative recombination losses reduction. The integrated incident photon to current efficiency, IPCE, is plotted in Fig. 5c. There is a good agreement between the integrated IPCE current, Fig. 5c, and the measured J_{SC}, Fig. 5b, with the highest photocurrent obtained also for cells with $NaBH_4$.

The initial power conversion efficiency for the reference cell (without borohydrides) was 15.7% with 21.8 mA cm^{-2} J_{SC}, 1.0 V V_{OC}, and 74% FF. However, the efficiency of cells improves with the addition of borohydrides. In the case of the KBH_4 added cell, the FF increases to 76% with an efficiency of 16.5%. In contrast, $NaBH_4$ cells improved all parameters, such as a V_{OC} of 1.1 V, a J_{SC} of 22.3 mA cm^{-2}, an FF of 78%, and a PCE of 17.7%. Solar cell performance values as summarized in Fig. S4 and Table S2. As demonstrated in seminal studies on methylammonium-free perovskites, Cs/FA-based compositions prioritize phase stability and long-term operational durability, particularly on planar n–i–p architectures.[37] While these systems can reach very high efficiencies under optimized conditions, their intrinsic crystallization kinetics and defect

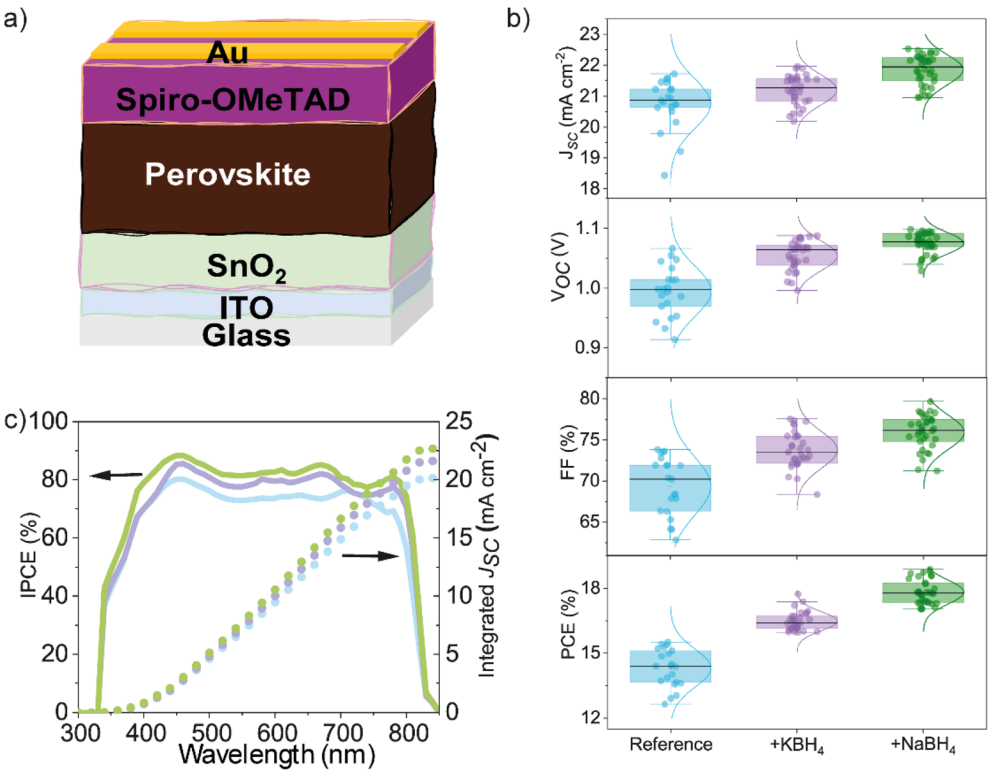

Fig. 5 (a) Solar cell architecture; (b) photovoltaic performance showing J_{SC}, V_{OC}, FF, and PCE with statistical analysis and (c) IPCE spectra and integrated current density of aged solar cells. The statistical analysis was collected from ~20 devices after 3 months of aging. The devices were stored under dark in a dry box under conditions of 20% RH and 25 °C.

tolerance generally result in lower initial PCEs compared to MA-containing compositions, which have achieved record efficiencies but often reduces thermal and ambient stability.[38] However, $Cs_{0.1}FA_{0.9}PbI_3$ formulation was intentionally selected to suppress phase instability and volatile cation-related degradation pathways. Therefore, efficiency is limited by stability-oriented design more than optimization for maximum initial performance. Accordingly, the primary contribution of this work leads in demonstrating significant improvements in long-term device stability, reinforcing the relevance of stability-driven compositional engineering practical perovskite solar cells.

Devices incorporating both borohydrides exhibit higher efficiencies than reference. This improvement results from their similar redox chemistry as the borohydride anion (BH_4^-) maintains perovskite stability by reducing I_2 to I^-. In addition, BH_4^- can coordinate with Pb^{2+}, enhancing the interface between the ETL and the perovskite layer.[20] Furthermore, the Na^+ cation contributes to stabilization within the perovskite structure and improves surface properties by promoting the growth of larger grains.[19] Due to its smaller ionic radius and higher electronegativity, Na^+ forms stronger interactions within the crystal lattice improving electronic quality and long-term chemical stability of the perovskite.

In contrast, the lower performance and reduced stability observed in devices containing KBH_4 may be attributed to the K^+ ion, which according to previous studies is not completely incorporated into the crystal lattice and can induce phase segregation. Moreover, K^+ reacts more readily with oxygen accelerating structural degradation (Fig. 6).[39]

The fabricated solar cells present and outstanding shelf stability under dark in a dry box under conditions of 20% RH and 25 °C in all the cases, even for reference sample, reporting a performance after close to 3000 h higher than the initial performance, see Fig. S5. The increase in efficiency is higher for samples with borohydrides, being the highest the obtained with $NaBH_4$ additive. These results are especially significant considering that the analyzed devices were unencapsulated. After this first stability analysis a harsher aging study of complete unencapsulated solar cell devices was performed exposing fresh devices to higher relative humidity (~60%) in oxygen atmosphere and measured weekly over 5 weeks, see Fig. 6. All *J–V* curves are presented in Fig. 6a–c, while photovoltaic parameters are summarized in Table S3. Note that in these conditions reference devices exhibited a continuous decrease in efficiency with aging, see Fig. 6d, retaining less than 80% of their initial performance after 168 hours of continuous operation, followed by complete degradation after 500 hours. In contrast, the devices incorporating borohydride showed an increase in their initial efficiency over time in both cases, without any signs of degradation until after 750 hours of operation, showing in fact higher performance than fresh samples, reaching even 20.1% PCE for $NaBH_4$ samples, see Table S3. After this time a decrease in efficiency is observed for samples with borohydride additives. Specifically, the device treated with KBH_4 exhibited a decline in PCE to below 70% of its initial value after 900 hours. Meanwhile, the device incorporating $NaBH_4$ showed only a slight reduction in PCE, maintaining over 90% of its initial efficiency after 900 hours. Previous studies have demonstrated that perovskite solar cells can exhibit aging-induced performance recovery even under dark storage, driven by slow interfacial equilibration, redistribution of mobile ionic species, and gradual defect passivation.[40,41] These processes can reduce non-radiative recombination and improve charge extraction, leading to increases in V_{OC} and FF over intermediate aging times. In our case, the presence of borohydrides on device enhances these benign aging effects by promoting continued passivation under suppressing recombination and reduce defects as shown in the Fig. 6d. As a result, an improvement in device performance is observed over long-term stability. All *J–V* measurements were performed under identical and reproducible conditions, confirming that the PCE increase at 720 hours reflects intrinsic device.

On other hand, we evaluated the operational stability of the unencapsulated devices control devices, KBH_4 and $NaBH_4$, respectively in demanding ambient conditions (~43% RH and 25 °C), tracking their performance at maximum power point (MPP) under continuous illumination (100 mW cm^{-2}, AM 1.5G) (Fig. S6). The control and KBH_4 device experienced a fast degradation, with a T_{80} lifetime of 7 and 14 hours. Conversely, $NaBH_4$ devices demonstrated significantly enhanced stabilities, achieving impressive T_{80} lifetimes more of 24 hours. Herein, we demonstrated a improvement in the ambient T_{80} lifetime, anticipating an outstanding stability without encapsulation. This achievement is particularly significant because, with $NaBH_4$ enhance V_{OC} and improve the operational stability at MPP.

In general, both $NaBH_4$ and KBH_4 exhibit excellent redox and structural stabilization properties. However, $NaBH_4$ demonstrates superior chemical compatibility and effectiveness in perovskite, as it efficiently restores I^- species through strong reduction by maintaining iodine in its reduced form. Furthermore, $NaBH_4$ also reduces the non-radiative carrier recombination which improve dramatically the resistance of device to humidity, see more details in Table S6.

On the other hand, to assess the impact of the additive in the recombination mechanisms,[42] the different devices' ideality factor, *n*, was calculated considering the relationship:

$$eV_{OC} = E_g + nk_BT\ln(\Phi/\Phi_0) \quad (3)$$

where *e* is the electron charge, E_g is the light absorber bandgap, k_B is the Boltzmann constant, *T* is the temperature, Φ is the light intensity and Φ_0 is a constant with the same units as Φ. *n* is a parameter related to recombination mechanism. Comparing *n* value of different samples at different aging stages helps to track and compare recombination mechanism evolution. In our case, this analysis, see Fig. 7 and Tables S5–S7, has been carried out on samples used for the stability characterization reported in Fig. 6, exposed to high relative humidity (RH ~ 60–25 °C%) in dark conditions. The measurements indicate that fresh devices, KBH_4, $NaBH_4$ and reference, exhibit similar behavior, see Fig. 7a. For fresh devices, KBH_4 exhibits an initial *n* value lower than 2, indicating a contribution of surface recombination to

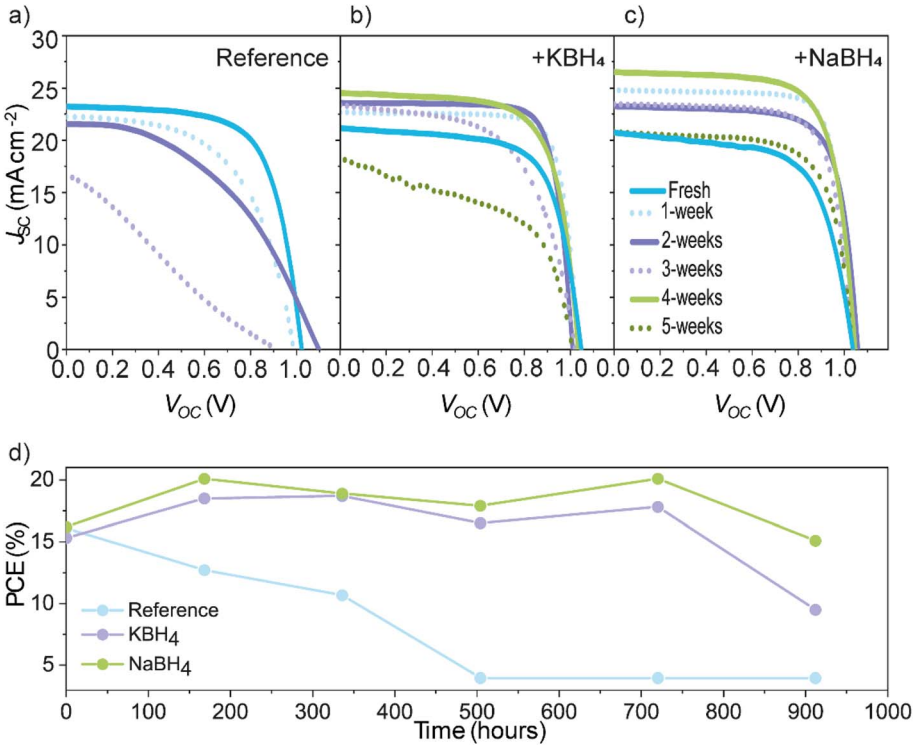

Fig. 6 *J–V* curve (a) reference, (b) KBH_4, (c) $NaBH_4$, and (d) the long-term stability of the perovskite solar cells was measured in ambient air exposed to high relative humidity (RH ~ 60–25 °C%) at dark conditions, measured every week for a period of 5 weeks.

the dominant bulk Shockley–Read–Hall (SRH) recombination. However, a lower n does not necessarily guarantee superior device performance or long-term stability.[43] In our case, fresh $NaBH_4$ device shows a slightly higher n than KBH_4, see Fig. 7a and Table S4, while simultaneously exhibiting a higher V_{OC}. This behavior suggests that recombination with $NaBH_4$ device is initially dominated by SRH recombination. However, aging could produce that Na^+ in electrically neutralizing bulk defects increasing the weight of interfacial recombination in the total recombination, reflected as a decrease of n.

Note that after two weeks, see Fig. 7b, borohydride aged samples slightly decrease the n values indicating the presence of an alternative interfacial recombination pathway. When interfacial recombination is the main recombination pathway an ideality factor of 1 is expected.[42] n values between 1 and 2 indicate the presence of both surface and bulk recombination. In contrast, n values higher than 2 points to multiple trapping recombination.[44] We have previously observed in outdoors aged perovskite minimodules that when initial n values between 1 and 2 evolves with aging time to $n > 2$ an irreversible degradation is experienced in the devices.[44] Similar effect is observed here. After 1 week reference cells show a $n > 2$, see Table S4 and Fig. 7b. It is needed to wait 5 weeks to observe the irreversible degradation, with $n > 2$ for KBH_4 sample, see Table S4 and Fig. 7b. In contrast, $NaBH_4$ sample still preserving $n < 2$ after this time exhibiting the highest stability. This analysis clearly

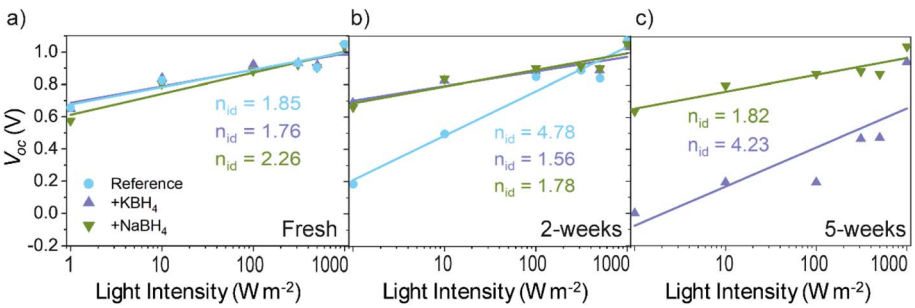

Fig. 7 Open-circuit potential *versus* light-intensity including ideality factors. Calculation of n_{id} from the relationship between the open-circuit voltage and the irradiance level, where the black lines correspond to fits in accordance with eqn (2) in SI. These data indicate that (a) $n_{id} = 1.85$ reference, 1.76 and 2.26 to KBH_4 and $NaBH_4$ fresh device; (b) $n_{id} = 4.78$ reference, 1.56 and 1.78 to KBH_4 and $NaBH_4$ device after 2-weeks of aging and (c) $n_{id} = 4.23$ and 1.86 to KBH_4 and $NaBH_4$ device after 5-weeks of aging.

establishes the beneficial role for perovskite solar cells stability of borohydride additives, especially in the case of $NaBH_4$, that also presents the less defective samples.

Conclusion

In summary, we demonstrate that two reducing agents, KBH_4 and $NaBH_4$, prevent the oxidation of the perovskite precursors within the solution, specifically by reducing iodine (I_2) to iodide (I^-). These agents stabilize the precursor solution and enhance stability in the solid state by passivating surface defects. This effect was demonstrated in the beneficial impact on photoconversion efficiency and long-term stability of the devices prepared with reducing agents. Incorporating the additives KBH_4 and $NaBH_4$ enhances the properties of the perovskite films by increasing their crystallinity and grain size, effectively decreasing non-radiative recombination. The increase of perovskite thin film properties is translated to the solar cell devices fabricated where devices prepared with borohydride additives presents higher performance especially when $NaBH_4$ is used. Concretely, the most dramatic increase respect the reference devices without additives in observed in the long-term stability of unencapsulated $CsFAPbI_3$-based devices with $NaBH_4$ additive in ambient high relative humidity RH 60% at 25 °C. Shelf stability in these conditions exceeds 900 hours after fabrication more than a 5-fold increase respect the reference devices. This work provides a simple and efficient strategy to improve the performance of PSCs, which will benefit future commercialization.

Conflicts of interest

There are no conflicts to declare.

Data availability

Data for this article, are available at zenodo repository at https://doi.org/10.5281/zenodo.15796891.

Supplementary information (SI) is available. See DOI: https://doi.org/10.1039/d5se01476j.

Acknowledgements

T. D. P would like to acknowledge her grant PREP2022-000274 PART OF PID2022-141683NB-I00, funded by MCIN/AEI/10.13039/501100011033 and by "ESF Investing in your future." S. H. T. C. gratefully acknowledges funding from the Ministry of Science and Innovation of Spain under Ayudas Ramón y Cajal (RYC2022-035578-I). E. M. B. B. acknowledges project EPCESBI – UJI-B2022-08. This work is partially funded by the European Union. Views and opinions expressed are however those of the author(s) only and do not necessarily reflect those of the European Union or the European Climate, Infrastructure and Environment Executive Agency. Neither the European Union nor the granting authority can be held responsible for them. HEPAFLEX project has received funding from HORIZON Research and Innovation Actions under grant Agreement no. 101122345. This work was supported by the Spanish Agencia Estatal de Investigación (AEI) and the Ministerio de Ciencia, Innovación y Universidades under grant PID2023-151880OB-C33 ConFlex project.

References

1 L. Gu, *et al.*, Boosting Stability of Cesium/Formamidinium Based Perovskite Solar Cells via Eliminating Intermediate Phase Transition and X-Anion Vacancy, *ACS Appl. Mater. Interfaces*, 2024, **17**, 991–1000, DOI: 10.1021/acsami.4c16316.
2 S. H. Turren-Cruz, A. Hagfeldt and M. Saliba, Methylammonium-free, high-performance and stable perovskite solar cells on a planar architectute, *Science*, 2018, **3583**(6413), 449–453, DOI: 10.1126/science.aat3583.
3 R. Sharif, *et al.*, A comprehensive review of the current progresses and material advances in perovskite solar cells, *Nanoscale Adv.*, 2023, **5**, 3803–3833, DOI: 10.1039/d3na00319a.
4 F. Zhang and K. Zhu, Additive Engineering for Efficient and Stable Perovskite Solar Cells, *Adv. Energy Mater.*, 2020, **10**(13), 1902579, DOI: 10.1002/aenm.201902579.
5 E. Ochoa-Martinez, *et al.*, Physical Passivation of Grain Boundaries and Defects in Perovskite Solar Cells by an Isolating Thin Polymer, *ACS Energy Lett.*, 2021, **6**(7), 2626–2634, DOI: 10.1021/acsenergylett.1c01187.
6 Y. Wu, *et al.*, Realizing High-Efficiency Perovskite Solar Cells by Passivating Triple-Cation Perovskite Films, *Sol. RRL*, 2022, **6**(7), 1–8, DOI: 10.1002/solr.202200115.
7 Y. Lu, *et al.*, Stabilization of Organic Cations in Lead Halide Perovskite Solar Cells Using Phosphine Oxides Derivatives, *J. Am. Chem. Soc.*, 2024, **146**(32), 22387–22395, DOI: 10.1021/jacs.4c05398.
8 A. F. V. Fonseca, *et al.*, In Situ PL Tracking of Halide Exchange at 3D/QD Heterojunction Perovskite Solar Cells, *ACS Energy Lett.*, 2024, **9**, 3177–3186.
9 S. P. Dunfield, *et al.*, From Defects to Degradation: A Mechanistic Understanding of Degradation in Perovskite Solar Cell Devices and Modules, *Adv. Energy Mater.*, 2020, **10**(26), 1–35, DOI: 10.1002/aenm.201904054.
10 M. Saliba, *et al.*, Cesium-containing triple cation perovskite solar cells: Improved stability, reproducibility and high efficiency, *Energy Environ. Sci.*, 2016, **9**(6), 1989–1997, DOI: 10.1039/C5EE03874J.
11 D. Prochowicz, *et al.*, Engineering of Perovskite Materials Based on Formamidinium and Cesium Hybridization for High-Efficiency Solar Cells, *Chem. Mater.*, 2019, **31**(5), 1620–1627, DOI: 10.1021/acs.chemmater.8b04871.
12 M. Li and C. Chen, The Aging Chemistry of Perovskite Precursor Solutions, *J. Phys. Chem. Lett.*, 2025, **16**(3), 754–765, DOI: 10.1021/acs.jpclett.4c03203.
13 J. Hu, *et al.*, Triiodide Attacks the Organic Cation in Hybrid Lead Halide Perovskites: Mechanism and Suppression, *Adv. Mater.*, 2023, **35**(40), 1–8, DOI: 10.1002/adma.202303373.
14 T. Kittikool, *et al.*, 120-Day perovskite solution stability via deprotonation and iodine reduction by a pyrazolone-based

additive, *Sol. Energy Mater. Sol. Cells*, 2025, **285**, 1–10, DOI: 10.1016/j.solmat.2025.113545.
15 L. Zhang, *et al.*, Strain Regulation and Defect Passivation of FA-Based Perovskite Materials for Highly Efficient Solar Cells, *Adv. Sci.*, 2024, **11**(7), 1–11, DOI: 10.1002/advs.202305582.
16 W. Hu, *et al.*, Stabilizing perovskite precursors with the reductive natural amino acid for printable mesoscopic perovskite solar cells, *J. Energy Chem.*, 2024, **90**, 32–39, DOI: 10.1016/j.jechem.2023.10.022.
17 K. Nagasawa, *et al.*, Improving the Photovoltaic Properties and Stability of Inverted Perovskite Solar Cells with Hydroxylamine-Based Additives, *Adv. Mater. Interfaces*, 2024, **11**(3), 1–9, DOI: 10.1002/admi.202300449.
18 K. Gao, *et al.*, Towards highly efficient and stable perovskite solar cells: Suppressing ion migration by inorganic boric acid stabilizer, *Nano Energy*, 2025, **133**, 1–7, DOI: 10.1016/j.nanoen.2024.110473.
19 J. Sanchez-Diaz, *et al.*, Tin perovskite solar cells with >1,300 h of operational stability in N2 through a synergistic chemical engineering approach, *Joule*, 2022, **6**, 861–883, DOI: 10.1016/j.joule.2022.02.014.
20 X. Wu, *et al.*, Exceeding 20% Efficiency for Highly Efficient and Stable Inverted Perovskite Solar Cells via Sodium Borohydride Induced Interface Engineering, *Sol. RRL*, 2023, **7**(1), 1–11, DOI: 10.1002/solr.202200833.
21 Y. Liu, *et al.*, Synergistic Redox Modulation for High-Performance Nickel Oxide-Based Inverted Perovskite Solar Modules, *Adv. Sci.*, 2024, **11**(21), 1–9, DOI: 10.1002/advs.202309111.
22 S. Chen, X. Xiao, H. Gu and J. Huang, Iodine reduction for reproducible and high-performance perovskite solar cells and modules, *Sci. Adv.*, 2021, **7**(10), 1–6, DOI: 10.1126/sciadv.abe8130.
23 H. Cheng, *et al.*, KBF4 Additive for Alleviating Microstrain, Improving Crystallinity, and Passivating Defects in Inverted Perovskite Solar Cells, *Adv. Funct. Mater.*, 2022, **32**(36), 1–9, DOI: 10.1002/adfm.202204880.
24 F. Li, K. Liu and J. Dai, Flexible p-i-n perovskite solar cell with optimized performance by KBF 4 additive, *Opt. Express*, 2024, **32**(1), 366–378, DOI: 10.1364/OE.503856.
25 J. Zhang, S. Wu, T. Liu, Z. Zhu and A. K. Y. Jen, Boosting Photovoltaic Performance for Lead Halide Perovskites Solar Cells with BF4− Anion Substitutions, *Adv. Funct. Mater.*, 2019, **29**(47), 1–8, DOI: 10.1002/adfm.201808833.
26 Y. Duan, *et al.*, 21.41%-Efficiency CsPbI3 Perovskite Solar Cells Enabled by an Effective Redox Strategy with 4-Fluorobenzothiohydrazide in Precursor Solution, *Adv. Funct. Mater.*, 2024, **34**(10), 1–10, DOI: 10.1002/adfm.202312638.
27 M. Li, *et al.*, Multifunctional Reductive Molecular Modulator toward Efficient and Stable Perovskite Solar Cells, *Sol. RRL*, 2021, **5**(10), 1–10, DOI: 10.1002/solr.202100320.
28 Y. Che, *et al.*, Hydrazide Derivatives for Defect Passivation in Pure CsPbI3 Perovskite Solar Cells, *Angew. Chem., Int. Ed.*, 2022, **61**(33), 1–8, DOI: 10.1002/anie.202205012.
29 J. Qi, *et al.*, Modulating Dual Functionalities of Hydrazide Derivatives for Iodide Oxidation Suppression and Defect Passivation in Printable Mesoscopic Perovskite Solar Cells, *Adv. Energy Mater.*, 2024, **14**(47), 1–9, DOI: 10.1002/aenm.202402344.
30 M. Li, *et al.*, Stabilizing Perovskite Precursor by Synergy of Functional Groups for NiOx-Based Inverted Solar Cells with 23.5 % Efficiency, *Angew. Chem., Int. Ed.*, 2022, **61**, 1–12, DOI: 10.1002/anie.202206914.
31 K. M. M. Salim, *et al.*, Boosting Long-Term Stability of Pure Formamidinium Perovskite Solar Cells by Ambient Air Additive Assisted Fabrication, *ACS Energy Lett.*, 2021, **6**, 3511–3521.
32 K. Ho, M. Wei, E. H. Sargent and G. C. Walker, Grain Transformation and Degradation Mechanism of Formamidinium and Cesium Lead Iodide Perovskite under Humidity and Light, *ACS Energy Lett.*, 2021, **6**, 934–940.
33 D. H. Kang, Y. J. Park, Y. S. Jeon and N. G. Park, Extended X-ray absorption fine structure (EXAFS) of FAPbI3 for understanding local structure-stability relation in perovskite solar cells, *J. Energy Chem.*, 2022, **67**, 549–554, DOI: 10.1016/j.jechem.2021.10.028.
34 M. Stolterfoht, *et al.*, Voltage-Dependent Photoluminescence and How It Correlates with the Fill Factor and Open-Circuit Voltage in Perovskite Solar Cells, *ACS Energy Lett.*, 2019, **4**, 2887–2892, DOI: 10.1021/acsenergylett.9b02262.
35 T. Kirchartz, J. A. Márquez, M. Stolterfoht and T. Unold, Photoluminescence-Based Characterization of Halide Perovskites for Photovoltaics, *Adv. Energy Mater.*, 2020, **10**(26), 1–21, DOI: 10.1002/aenm.201904134.
36 F. Ma, *et al.*, Stable α/δ phase junction of formamidinium lead iodide perovskites for enhanced near-infrared emission, *Chem. Sci.*, 2016, **8**, 800–805, DOI: 10.1039/c6sc03542f.
37 H. Turren-Cruz, A. Hagfeldt and M. Saliba, Methylammonium-Free High-Performance, and Stable Perovskite Solar Cells on a Planar Architecture, *Science*, 2018, **362**(6413), 449–453, DOI: 10.1126/science.aat358.
38 S. Wang, *et al.*, Over 24% efficient MA-free CsxFA1−xPbX3 perovskite solar cells, *Joule*, 2022, **6**, 1344–1356, DOI: 10.1016/j.joule.2022.05.002.
39 D. J. Kubicki, *et al.*, Phase Segregation in Cs-, Rb- and K-Doped Mixed-Cation (MA)x(FA)1–xPbI3 Hybrid Perovskites from Solid-State NMR, *J. Am. Chem. Soc.*, 2017, **139**(40), 14173–14180, DOI: 10.1021/jacs.7b07223.
40 D. G. Lee, *et al.*, Effect of Metal Electrodes on Aging-Induced Performance Recovery in Perovskite Solar Cells, *ACS Appl. Mater. Interfaces*, 2019, **11**(51), 48497–48504, DOI: 10.1021/acsami.9b14619.
41 W. Zhu, *et al.*, Ion Migration in Organic–Inorganic Hybrid Perovskite Solar Cells: Current Understanding and Perspectives, *Small*, 2022, **18**(15), 1–16, DOI: 10.1002/smll.202105783.
42 W. Tress, *et al.*, Interpretation and evolution of open-circuit voltage, recombination, ideality factor and subgap defect states during reversible light-soaking and irreversible

degradation of perovskite solar cells, *Energy Environ. Sci.*, 2018, **11**, 151–165.

43 E. L. Unger, A. Czudek, H. S. Kim and W. Tress, Current-Voltage Analysis: Lessons Learned from Hysteresis, *Characterization Techniques for Perovskite Solar Cell Materials*, 2019, DOI: 10.1016/B978-0-12-814727-6.00004-9.

44 E. Velilla, F. Jaramillo and I. Mora-Seró, High-throughput analysis of the ideality factor to evaluate the outdoor performance of perovskite solar minimodules, *Nat. Energy*, 2021, **6**(1), 54–62.